NASA Technical Memorandum 79216

REDUCTION OF PARTICULATE CARRYOVER FROM A PRESSURIZED FLUIDIZED BED

R. W. Patch
Lewis Research Center
Cleveland, Ohio

Prepared for the
Second Symposium on the Transfer and Utilization
of Particulate Control Technology
Denver, Colorado, July 23-27, 1979

REDUCTION OF PARTICULATE CARRYOVER FROM A PRESSURIZED FLUIDIZED BED

By:

R. W. Patch
National Aeronautics and Space Administration
Lewis Research Center
Cleveland, Ohio 44135

ABSTRACT

A bench-scale fluidized-bed combustor was constructed with a conical shape so that the enlarged upper part of the combustor would also serve as a granular bed filter. The combustor was fed coal and limestone. Ninety-nine tests of about four hours each were conducted over a range of conditions. Coal-to-air ratio varied from 0.033 to 0.098 (all lean). Limestone-to-coal ratio varied from 0.06 to 0.36. Bed depth varied from 3.66 to 8.07 feet. Temperature varied from 1447 to 1905 F. Pressure varied from 40 to 82 psia. Heat transfer area had the range zero to 2.72 ft^2. Two cone angles were used. The average particulate carry-over of 2.5 grains/SCF was appreciably less than cylindrical fluidized-bed combustors. The carry-over was correlated by multiple regression analysis to yield the dependence on bed depth and hence the collection efficiency, which was 20%. A comparison with a model indicated that the exhaust port may be below the transport disengaging height for most of the tests, indicating that further reduction in carry-over and increase in collection efficiency could be affected by increasing the freeboard and height of the exhaust port above the bed.

INTRODUCTION

The pressurized fluidized-bed combustor (PFBC) is being investigated by the Department of Energy, the utility industry, and several laboratories with the ultimate purpose of achieving clean coal combustion in high-efficiency central-station power plants. Not only must the flue gas meet EPA New Source Performance Standards for particulate and other emissions, but the power plant cycles require gas turbines to recover energy from the hot, pressurized flue gas, and these turbines will not tolerate large quantities of particulates in the gas driving the turbine. Also, the carry-over of unburned carbon must be reduced or recycled to achieve acceptable combustion efficiency. The state of the art at present in research PFBC's is to provide one to three stages of high-temperature cyclones and perhaps an additional clean-up device downstream. The solids from the high-temperature cyclones usually are recycled to the bed or go to a carbon burn-up cell to improve the combustion efficiency of the system. Unfortunately, the high-temperature cyclones frequently are not very reliable due to erosion and seal problems, as mentioned by Rollbuhler (1979)[1].

The primary purpose of the present program at Lewis is to test turbine blade materials in PFBC flue gas. It was also hoped that by making the

combustor conical in shape so that the gas velocity at the top of the bed was greatly reduced, the particulate carry-over (solids loading) could be significantly reduced. Hence, the number of high temperature cyclones and carbon burn-up cells in a larger scale combustor could be reduced and the erosion of any remaining cyclones minimized. This appeared feasible because most of the combustion occurs near the bottom of a PFBC as evidenced by the axial temperature profile, and the top is mostly used for SO_2 adsorption, NO_x reduction, and possibly heat transfer tubes. Hence, the top, if enlarged, can serve as an in-bed granular filter for particulates. This paper is a report on this phase of the project and describes the first conical PFBC built anywhere.

APPARATUS

The Lewis PFBC is shown schematically in Figure 1 and has a conical shape to reduce the gas velocity at the top of the bed. The combustor has a carbon steel exterior lined with Kaowool insulation which, in turn, is lined with cast ceramic insulation.

The combustor is fed a mixture of coal and limestone (fuel). The coal and limestone storage hoppers feed metering screws which feed a blending auger. The blended fuel mixture flows from the blending auger to a fuel holding hopper at atmospheric pressure. The fuel holding hopper is used to pressurize the fuel up to bed pressure. The fuel is intermittently dumped at pressure into the pressurized fuel feed hopper. The fuel feed hopper feeds the bed continuously with the help of the fuel metering screw and a small supply of high pressure air as a transport medium.

The main air supply for the bed was dry air at ambient temperature monitored by a venturi flowmeter. It flowed into the bottom of the combustor through a distributor containing nine bubble caps, each with four 1/8 inch diameter holes.

The bed consisted mostly of limestone products and ash. The bed height was controlled by a discharge solids removal auger, which could be located at one of six ports at different heights. The removal auger was rotated continuously so that the bed level never exceeded its height.

Two geometries were used for the bed (Figure 2). For tests 1 to 29 the bed had a 3.40° half angle, and the gas temperatures at the exhaust port were much lower than the bed temperatures. For tests 30 to 99 the upper side and top insulation were increased to minimize this heat loss. This reduced the bed half angle to 2.51°.

To determine the amount of particulates in the flue gas, about one-fourth of the flow was bypassed through cyclone separator number 6 and a stainless steel mesh filter with a 0.5 micron nominal rating and then through a venturi flowmeter before venting to the atmosphere.

Additional details of the system and its instrumentation are given by Kobak (1979)[2]. The scale and general arrangement of the PFBC system can be seen from Figure 3.

EXPERIMENTAL PROCEDURE

A high-volatile coking bituminous coal from the Pittsburgh #8 seam was used in the tests described here. Typical ultimate and proximate analyses are given in Table 1. The coal was pulverized, and the -7 mesh fraction used without drying. It had an approximately 800 micron median diameter (50th weight percentile).

The limestone was from Grove City, Virginia, and had a size of -7 +18 mesh, yielding an approximately 1600 micron median diameter. The size distribution is given in Figure 4 and composition in Table 2. It was used without drying.

The bed initially consisted of the mixture of limestone products and ash left over from the bed of previous tests. This reduced the time required for the bed to reach chemical equilibrium during a test.

Each test was about four hours duration. Starting and operating procedures are given by Kobak (1979)[2]. During the last two hours the particulate loading of the exhaust gas was measured by means of separator number 6, the mesh filter, and the venturi flowmeter (Figure 1). The particulates from separator number 6 and the mesh filter were collected and weighed.

RESULTS AND DISCUSSION

The following sections give the test conditions, size distributions of particles, compositions of effluents, multiple regression analyses for solids loading, filter efficiency, comparisons and explanation of solids loading, and bed pressure drop.

Test Conditions, Size Distributions and Compositions of Effluents

Ninety-nine tests were run. The first 29 had a cone half angle, a (symbols are given in Appendix A), of 3.4^{0}; whereas, the last seventy had a cone half angle of 2.5^{0} (see Figure 2). There were six other degrees of freedom in the experiment. Consequently, six other independent variables besides a were needed to specify a test condition. There are various possible ways of choosing these six. For this paper, the other six were coal-to-air ratio c, limestone-to-coal ratio L, bed depth D, heat exchanger area S, bed pressure p, and gas velocity at the bottom of the bed V_b. These seven independent variables are enough to determine the bed temperature T, the gas velocity at the top of the bed V_t, the coal feed rate w_c, the excess air ratio E, and the calcium-to-sulfur molar ratio C_s, so that the last five are not independent. The ranges and averages of the independent variables and of T, V_t, w_c, E, and C_s are given in Table 3.

The solids loadings of the flue gas exiting the top of the combustor can be expressed in units of grains per standard cubic foot of gas (S_t) or in units of pounds per million British thermal units from the coal (S_b). The ranges and averages of these quantities are also given in

Table 3. The current New Source Performance Standard (NSPS) promulgated by EPA for large electric-utility boilers is given in Table 4. It can be seen that hot-gas clean-up would be needed to meet the NSPS, not to mention the requirements if a gas turbine were located downstream to recover energy from the pressurized flue gas.

An examination of the size distributions of the solids to and from the bed (Figure 4) gives an idea of what is taking place and the degree of attrition in the bed. The solids fed the bed are limestone and coal, but most of the coal burns away leaving coal ash. The particle size of the raw limestone is largest and narrowly distributed. Two curves are given for the coal ash. The right-hand curve is the distribution that would result if each coal particle contained one ash particle of the same weight fraction as the average for the coal. The left-hand curve was measured by dry and wet seiving coal ash produced by burning the coal at 1700 F for one hour in a laboratory furnace with adequate ventilation in a manner similar to Merrick and Highley (1974)[3]. The source of the solids removed from the bed was determined by using silicon as a tracer for coal ash and calcium as a tracer for limestone and is given in Figure 5 (only the average is shown for the minor constituents). The bed discharge was mostly limestone whereas the fly ash was mostly coal ash and char. Going back to Figure 4, it can be seen that there is appreciable attrition in the bed of limestone and perhaps coal ash.

Figure 6 shows the cumulative loading of the flue gas at the exit from the combustor in grains per standard cubic foot. The ordinate gives the loading by all particles up to the particle size given on the abscissa.

Loading and Filter Efficiency From Multiple Regression Analysis

The data from the 99 tests exhibited considerable scatter, and for the most part were not taken with the object of determining solids loading as a function of c, L, D, S, a, p, and V_b, but rather primarily with the object of determining gaseous emissions and combustion efficiency as functions of other sets of seven independent variables. To obtain maximum utilization of the data and confidence in the results, it was, therefore, necessary to use multiple regression analysis to correlate S_t and S_b with c, L, D, S, a, p, and V_b. This gave

$$S_t = 1.014 - 20.44L - 0.1140D + 0.5606S + 0.5498V_b + 73.89L^2 \qquad (1)$$

$$S_b = 4.278 - 40.47L - 0.2316D + 1.243V_b + 146.3L^2 \qquad (2)$$

The observed total solids loadings S_t and S_b are plotted versus equations (1) and (2), respectively, in Figures 7 and 8. Here the diagonal lines are the loci of perfect agreement.

If the reader wishes to use equations (1) and (2) where not all the independent variables L, D, S, and V_b are known, or if comparisons are to be made with a combustor of a different size so its value of S is not pertinent, the following relations from multiple regression analyses may be useful for estimating S and w_c for the conical PFBC:

$$S = 7.855 + 75.78c + 0.6197L + 0.125D - 0.008913T - 0.8183a + 0.04839p + 0.5312V_b \quad (3)$$

$$w_c = -49.57 + 241.2c + 5.019L + 0.08918D + 5.027S + 0.06709a + 0.4487p + 6.712V_b \quad (4)$$

It may be desirable to convert from coal-to-air ratio c to excess air ratio E. The stoichiometric value of c is 0.1004 for the coal used so

$$E = 0.1004/c - 1 \quad (5)$$

It may also be required to convert limestone-to-coal ratio L to calcium-to-sulfur molar ratio C_s, which can be accomplished for the coal and limestone used by means of

$$C_s = 15.58L \quad (6)$$

By making use of equations (1) and (3) it is possible to predict conical PFBC solids loadings for test conditions of cylindrical PFBC's at other laboratories. In doing this the excess air ratio, bed depth, bed temperature, bed pressure, and gas velocity at the bottom of the bed were assumed to be the same for conical and cylindrical PFBC's. The average cone half angle of 2.77° for the 99 tests was used for the conical PFBC. A comparison with the Leatherhead (1974)[4] PFBC is given in Table 5. The conical PFBC would have had 40 percent less solids loading. A comparison with the Argonne PFBC (using data from Montagna (1978)[5] and Swift (1979)[6]) is given in Table 6. The conical PFBC would have had 31 percent less solids loading.

Equation (1) may be used to produce a graph of solids loading and fractional collection efficiency of the top part of the fluidized bed considered as a filter. To do this, the average values of L, S, and V_b were assumed. The solids loading is shown in Figure 9 and decreases linearly with bed depth. If the lower 3.657 feet of the bed is regarded as the combustor and the part of the bed above 3.657 feet is regarded as the in-bed filter, the fractional collection efficiency η of the in-bed filter is readily calculated from

$$\eta(D) = 1 - S_t(D)/S_t(3.657) \quad (7)$$

and is also shown in Figure 9. The maximum collection efficiency was 20 percent.

Explanation for Solids Loadings and In-Bed Collection Efficiency

A theoretical investigation comprising two phases was undertaken to attempt to explain the low filter efficiency of the in-bed filter. The first phase was based on a theoretical model and computer programs by Horio, et al (1977)[7] as modified by Patch (1979)[8].

The model is summarized briefly below:

It is assumed that "fast" bubbles are present (rising velocity of bubble greater than gas velocity in emulsion). Hence, the bubbles have clouds. The bubble size is given by the correlation of Mori and Wen (1975)[9] modified for a combustor of varying cross-sectional area. Char and limestone are assumed to be completely mixed. Plug flow of gas is assumed.

A spherical particle model is employed for coal combustion. Only the lean case is treated. The hydrogen and oxygen volatize immediately upon injection of coal into the combustor, not changing the diameter of the resultant char. The diameter is gradually reduced by burning with oxygen, with the rate determined by the surface rate of chemical reaction and gas diffusion. Ash particles break off as the char burns. Carbon, nitrogen, and sulfur in the char are assumed to be released or used at the same rate as the char burns.

Elutriation of char, ash, and limestone are treated differently. For char it is assumed that the combustor exhaust gas port is above the transport disengaging height, and one of three empirical correlations (Zenz and Weil (1958)[10], Kunii and Levenspiel (1969)[11], Wen and Hashinger (1960)[12]) may be selected for the elutriation rate. The fraction of ash elutriated is not calculated so it must be given as an input. The limestone is assumed not to elutriate.

For comparison between the model and experiment, five steady-state tests (no. 100-104) with a total duration of 20 hours and 7 minutes were run under the same conditions with a bed depth D of 4.657 ft., and results were averaged. Since the model calculates the burnable carbon entrained but not ash or limestone entrained, comparison was based on burnable carbon entrained and is shown in Figure 10 for the three empirical elutriation correlations. Clearly the Horio et al model using the Zenz and Weil correlation agreed closest with experiment, but it predicted burnable carbon entrained more than an order of magnitude too low. In addition, the predicted diameter of the entrained burnable carbon was about a factor of three too high no matter which elutriation correlation was used (Figure 11).

To attempt to elucidate the discrepancies, comparisons were made between the model and tests 1 to 29 and are shown in Figure 12. Here it is significant that the calculated burnable carbon entrained fell off more rapidly with increasing bed depth than observed. Since increasing bed depth decreases freeboard (and exhaust port) height (see Figure 12) this divergence of trends would be explained if the combustor exit port were below the transport disengaging height so that bed material was being splashed into the exit port by bursting bubbles.

The second phase of the investigation was a comparison of empirical transport disengaging heights with the experimental freeboard and exit port heights. Unfortunately, no general empirical correlation of transport disengaging heights was available that did not require a special computer program. Three empirical correlations for cracking catalyst were available (Zenz and Weil (1958)[10], Amitin et al (1968)[13], and

Fournol et al (1973)[14]) and are plotted in Figure 13 along with freeboard height. The correlations all tend to indicate the freeboard height was less than the transport disengaging height, especially for a bed depth of 8.073 ft. This condition could be further aggravated because coal ash tends to have a particle density less than cracking catalyst, so its transport disengaging height would be even higher than the correlations in Figure 13. Hence, it is believed that if the freeboard height (and combustor exhaust port height) were increased substantially, while holding bed depth constant, S_t would decrease and apparent filter efficiency would increase markedly.

Bed Pressure Drop

Bed pressure drop for tests 1-99 are shown in Figure 14. The dependence of bed pressure drop on bed depth was approximately linear as expected. When the bed depth was increased from 3.657 ft. to 8.073 ft., the pressure drop increased from about 0.6 psi to 3.2 psi, so the pressure drop attributable to the in-bed filter was about 2.6 psi.

There were three causes for the scatter in Figure 14. (1) When the limestone-to-coal ratio L was increased, the fraction of the bed which was limestone increased. The remainder of the bed was mainly ash. Since limestone is denser than ash, Δp increased. (2) When the air velocity at the bottom V_b was increased, the bubble fraction increased. Since the bubbles had very little weight, Δp decreased. (3) There was inherent experimental scatter, partly due to sampling error (only about eight readings were taken per test).

The bed pressure drop does not appear to present any significant application problem.

SUMMARY OF RESULTS

Use of a conical combustor shape to produce an in-bed filter resulted in from 31 to 40 percent less solids loading of the flue gas at the combustor exhaust port compared to cylindrical pressurized fluidized bed combustors at other laboratories. Solids loading at the exhaust port of the conical PFBC was found to increase linearly with gas velocity at the bottom of the bed and with heat transfer area, decrease linearly with bed depth, and had a parabolic dependence on limestone-to-coal ratio. This resulted in a filter efficiency of 20 percent for the deepest bed. Additional hot gas clean-up would be necessary to meet EPA New Source Performance Standards for large electric-utility boilers and for a gas turbine.

An investigation into the cause of the poor filter efficiency indicated that the combustor exhaust port was probably below the transport disengaging height. Hence, a marked improvement in filter efficiency can probably be expected if the freeboard is increased so the combustor exhaust port can be raised.

The pressure drop attributable to the in-bed filter was about 2.6 psi, which does not appear to present any significant application problem.

APPENDIX A - SYMBOLS

a	bed half angle (see Figure 2), deg.
B	fraction of burnable carbon entrained
C_s	molar ratio of calcium in limestone fed to sulfur in coal fed
c	coal-to-air ratio, as received weight basis
D	bed depth, ft
d	particle diameter, μm
E	excess air ratio
H	freeboard height, ft
L	limestone-to-coal ratio, as received weight basis
p	absolute pressure at top of combustor, psia
S	area of outside of heat exchanger and extractor tubes, ft^2
S_b	flue gas solids loading (particulate carry-over) at outlet of combustor based on higher heating value of coal, $lb/10^6$ Btu
S_t	flue gas solids loading (particulate carry-over) at outlet of combustor, wet gas basis, gr/SCF
T	bed temperature 1.22 ft above distributor, F
V_b	superficial velocity at bottom of bed, ft/sec
V_t	superficial velocity at top of bed, ft/sec
w_c	coal feed rate, as received basis, lb/hr
Δd	difference in particle diameter between two adjacent sieve sizes
Δp	bed pressure drop, psi
ΔW	weight of particles with diameters between two adjacent sieve sizes
η	fractional collection efficiency of filter

REFERENCES

1 Rollbuhler, R. J. Variable Operating Characteristics of a Conical Pressurized, Fluidized Bed Research Reactor. NASA TM report (to be published).

2 Kobak, J. A. Burn Coal Cleanly in a Fluidized Bed. Instru. and Control Systems. 52:29-32, January 1979.

3 Merrick, D., and J. Highley. Particle Size Reduction and Elutriation in a Fluidized Bed Process. AIChE Symp. Series. 70:366-378, January 1974.

4 Annonymous. Pressurized Fluidized Bed Combustion. National Research Development Corporation, (London). OCR-85-Int-1, July 1974.

5 Montagna, J. C., G. W. Smith, F. G. Teats, G. J. Vogel, and A. A. Jonke. Evaluation of On-Line Light-Scattering Opitcal Particle Analyzers for Measurements at High Temperature and Pressure. Argonne National Laboratory (Ill.). ANL/CEN/FE-77-7, 1978.

6 Swift, W. M. Personal communication. May 1979.

7 Horio, M., P. Rengarajan, R. Krishnan, and C. Y. Wen. Fluidized Bed Combustor Modeling. NASA CR-135164, 1977.

8 Patch, R. W. Preliminary Comparison of Theory and Experiment for a Conical, Pressurized Fluidized Bed Coal Combustor. NASA TM-79137, 1979.

9 Mori, S., and C. Y. Wen. Estimation of Bubble Diameter in Gaseous Fluidized Beds. Am. Inst. Chem. Eng. J. 21:109-115, January 1975.

10 Zenz, F. A., and N. A. Weil. A Theoretical-Empirical Approach to the Mechanism of Particle Entrainment from Fluidized Beds. AIChEJ 4:472-479, December 1958.

11 Kunii, D., and O. Levenspiel. Fluidization Engineering. New York, Wiley and Sons, 1969, p. 313-317 (Primary Source - S. Yagi and T. Aochi. Paper presented at the Soc. of Chem. Engrs. (Japan), Fall Meeting, 1955).

12 Wen, C. Y., and R. F. Hashinger. Elutriation of Solid Particles from a Dense-Phase Fluidized Bed. AIChE J. 6:220-226, June 1960.

13 Amitin, A. V., I. G. Martyushin, and D. A. Gurevich. Dusting in the Space Above the Bed in Converters with a Fluidized Catalyst Bed. Chem. Technol. Fuels Oils. 3:181-184, 1968.

14 Fournol, A. B., M. A. Bergougnou, and C. G. J. Baker. Solids Entrainment in a Large Gas Fluidized Bed. Can. J. Chem. Eng. 51:401-404, August 1973.

TABLE 1. ULTIMATE AND PROXIMATE ANALYSIS OF PITTSBURG #8 COAL

ULTIMATE ANALYSIS (DRY BASIS)	
CARBON	75.38%
HYDROGEN	5.14
NITROGEN	1.49
CHLORINE	0.01
SULFUR	1.99
ASH	8.38
OXYGEN	7.61
	100.00%

PROXIMATE ANALYSIS (AS RECEIVED)	
MOISTURE	2.12%
ASH	8.20
VOLATILE MATTER	37.41
FIXED CARBON	52.27
	100.00%

HIGHER HEATING VALUE
13274 BTU/LB

TABLE 2. COMPOSITION OF GROVE LIMESTONE BY WEIGHT (DRY BASIS)

LIME	53.97%
CARBON DIOXIDE	43.42
SILICA	1.17
MAGNESIA	1.16
ALUMINA	0.14
FERRIC OXIDE	0.11
SULFUR	0.08
BURNABLE CARBON	0.08
UNDETERMINED	-0.13
	100.00%

TABLE 3. RANGES AND AVERAGES OF VARIABLES IN CONICAL PRESSURIZED FLUIDIZED - BED COMBUSTOR

VARIABLE*	MINIMUM (AVERAGED OVER 4 HR TEST)	MAXIMUM (AVERAGED OVER 4 HR TEST)	AVERAGE OF ALL TESTS
COAL-TO-AIR RATIO, c	0.0334	0.0977	0.0616
LIMESTONE-TO-COAL RATIO, L	0.064	0.364	0.138
BED DEPTH, D, FT	3.66	8.07	5.34
HEAT TRANSFER AREA, S, FT^2	0	2.72	1.68
CONE HALF ANGLE, θ, DEG.	2.51	3.40	2.77
BED PRESSURE, p, PSIA	39.7	82.2	72.5
GAS VELOCITY AT BOTTOM, V_b FT/SEC	2.20	8.58	4.39
BED TEMPERATURE, T, F.	1447	1905	1701
GAS VELOCITY AT TOP OF BED, V_t, FT/SEC	0.701	4.43	1.76
COAL FEED RATE, w_c, LB/HR	15.0	63.7	37.1
EXCESS AIR RATIO, E	0.028	2.01	0.630
CALCIUM-TO-SULFUR MOLAR RATIO, C_s	0.997	5.67	2.15
SOLIDS LOADING, S_t, GR/SCF	0.730	9.15	2.50
SOLIDS LOADING, S_b, $LB/10^6$ BTU	1.38	18.9	6.09
BED PRESSURE DROP, Δp, PSI	0.14	3.89	1.60

*SEE APPENDIX A FOR MORE COMPLETE DEFINITIONS

TABLE 4. COMPARISON OF SOLIDS LOADING AT COMBUSTOR EXIT AND NEW SOURCE PERFORMANCE STANDARDS FOR LARGE ELECTRIC UTILITY BOILERS

	SOLIDS LOADING S_b $LB/10^6$ BTU
MINIMUM (AVERAGED OVER 4 HR TEST)	1.38
MAXIMUM (AVERAGED OVER 4 HR TEST)	18.9
AVERAGE OF ALL TESTS	6.09
CURRENT EPA NEW SOURCE PERFORMANCE STANDARD	0.03

TABLE 5. COMPARISON OF SOLIDS LOADINGS AT COMBUSTOR EXIT WITH PFBC AT LEATHERHEAD (1974)[4] (USING EQUATIONS (1) AND (3) TO EXTRAPOLATE PFBC PERFORMANCE)

	EXPERIMENTAL QUANTITIES FOR CYLINDRICAL PFBC AT LEATHERHEAD (1974)[4]	PREDICTED QUANTITIES FOR CONICAL PFBC AT LEWIS (THIS PAPER)
EXCESS AIR RATIO, E	0.16	0.16
COAL-TO-AIR RATIO, c		0.0866
CALCIUM-TO-SULFUR MOLAR RATIO, Cs	2.03	2.03
LIMESTONE-TO-COAL RATIO, L		0.130
BED DEPTH, D, FT	4.1	4.1
BED TEMPERATURE, T, F	1740	1740
HEAT TRANSFER AREA*, S, FT^2		2.67
CONE HALF ANGLE, ϕ, DEG.	0	2.77
BED PRESSURE, p, PSIA	87	87
GAS VELOCITY AT BOTTOM, V_b, FT/SEC	2.3	2.3
SOLIDS LOADING, S_t, GR/SCF	3.16	1.90

*FROM EQUATION (3)

TABLE 6. COMPARISON OF SOLIDS LOADINGS AT COMBUSTOR EXIT WITH PFBC AT ARGONNE (USING EQUATIONS (1) AND (3) TO EXTRAPOLATE CONICAL PFBC PERFORMANCE)

	EXPERIMENTAL QUANTITIES FOR CYLINDRICAL PFBC AT ARGONNE	PREDICTED QUANTITIES FOR CONICAL PFBC AT LEWIS (THIS PAPER)
EXCESS AIR RATIO, E	0.15	0.15
COAL-TO-AIR RATIO, c		0.0873
LIMESTONE-TO-COAL RATIO, L	0.562	0.562
BED DEPTH, D, FT	3	3
BED TEMPERATURE, T, F	1561	1561
HEAT TRANSFER AREA*, S, FT^2		2.88
CONE HALF ANGLE, ϕ, DEG.	0	2.77
BED PRESSURE, p, PSIA	44.1	44.1
GAS VELOCITY AT BOTTOM, V_b, FT/SEC	3.28	3.28
SOLIDS LOADING, S_t, GR/SCF	23	15.9

*FROM EQUATION (3)

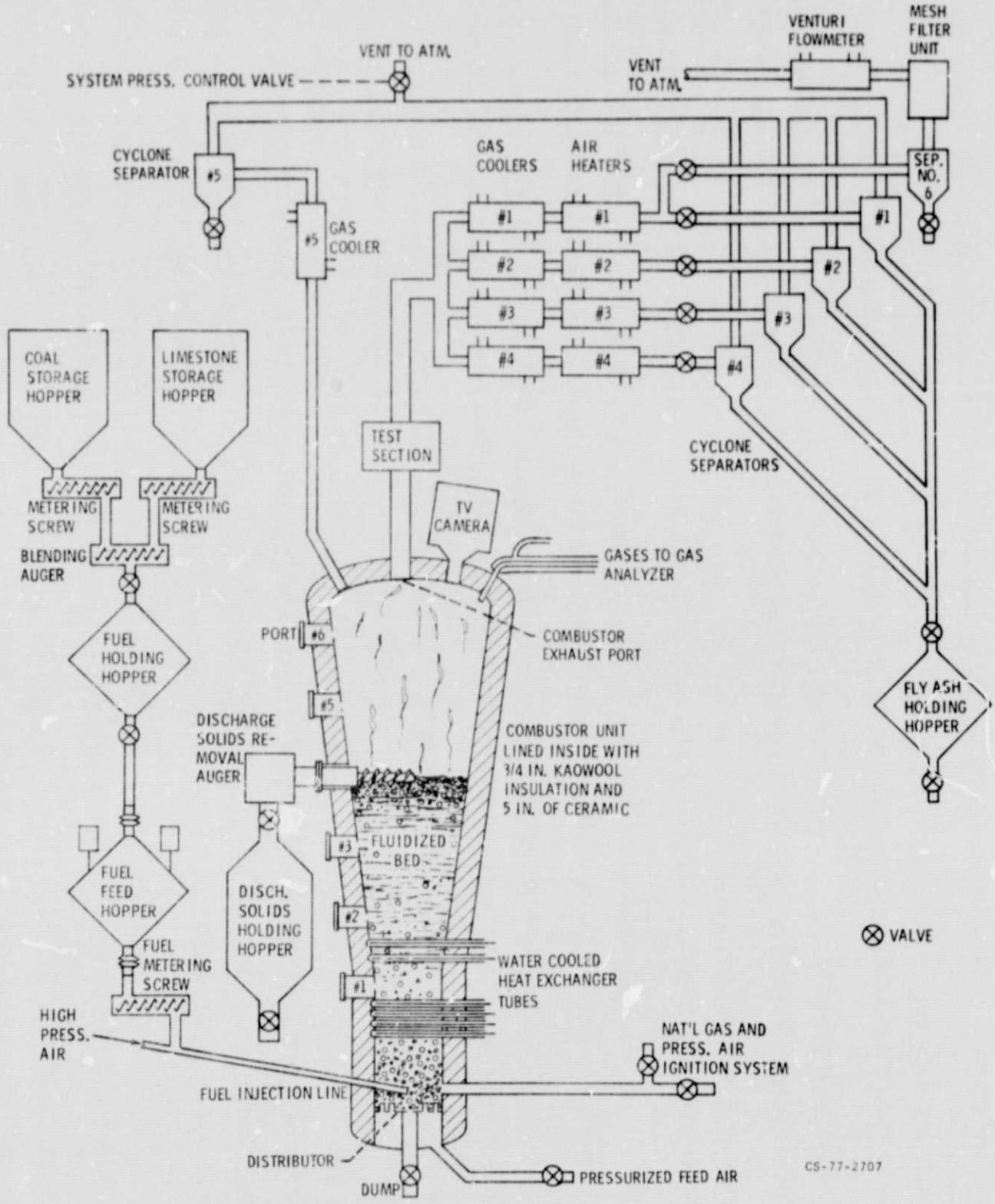

Figure 1 Schematic of LeRC pressurized fluidized bed combustor.

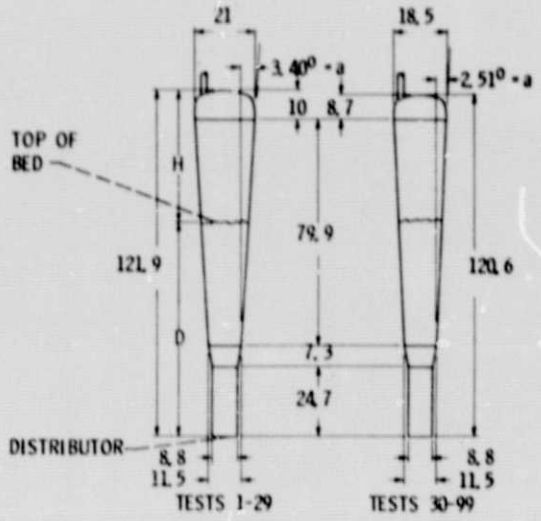

Figure 2 Two internal geometries of combustor (dimensions in inches except D and H; discharge solids removal auger and heat exchanger tubes omitted).

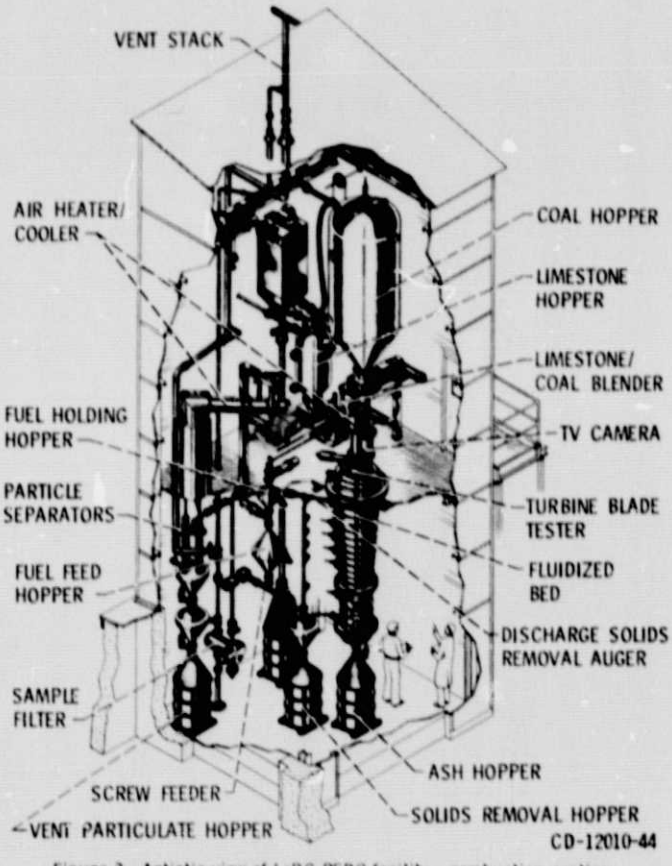

Figure 3 Artistic view of LeRC PFBC facility - combustion section.

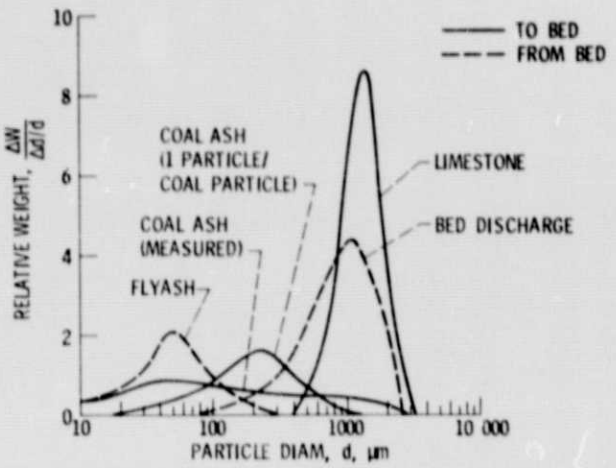

Figure 4 Solids size distributions.

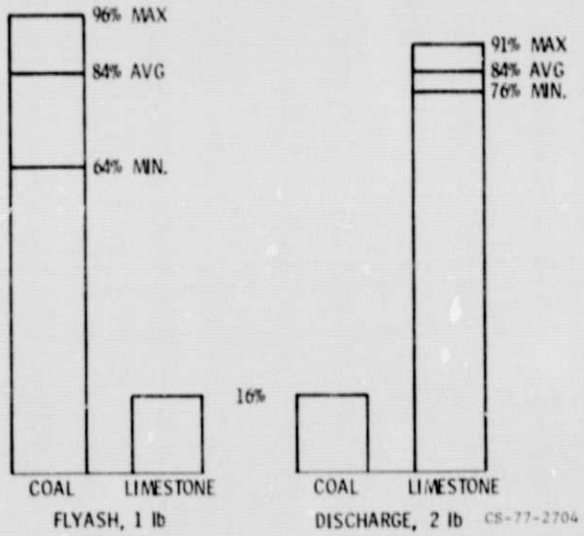

Figure 5 Source of solids removed from bed.

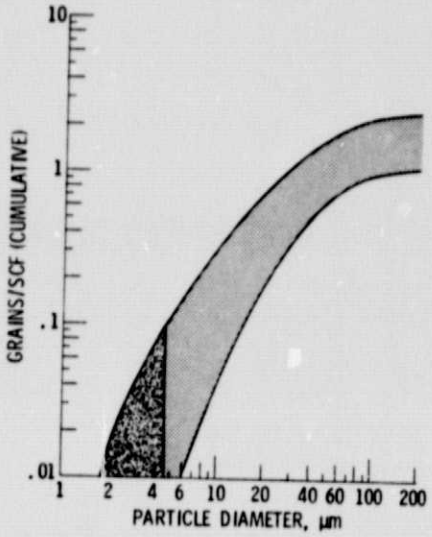

Figure 6 Particles in gases from combustor.

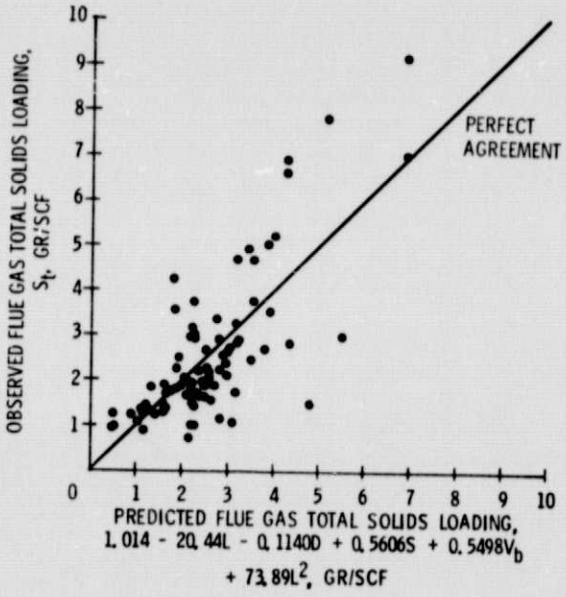

Figure 7 Comparison of observed flue gas total solids loading with predicted values.

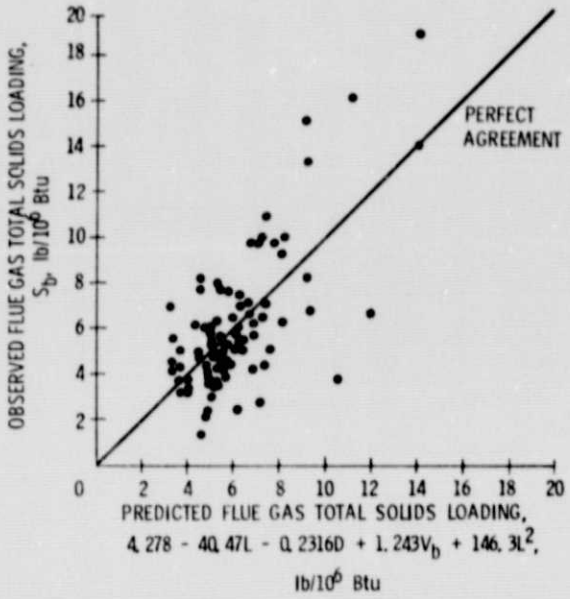

Figure 8 Comparison of observed flue gas total solids loading based on higher heating value with predicted values.

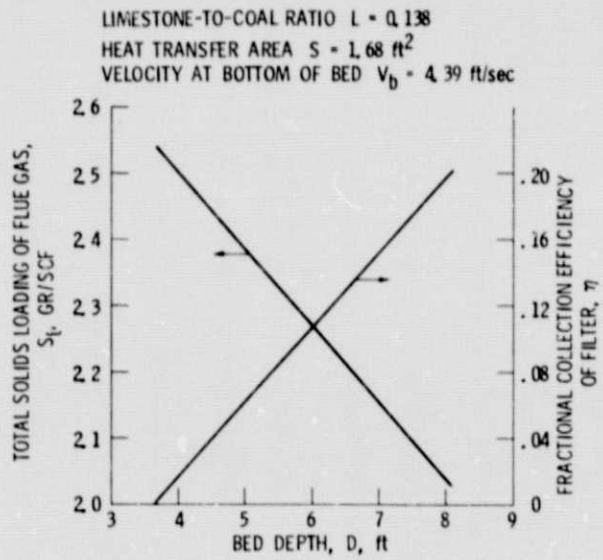

Figure 9 Total solids loading of flue gas at combustor exit and resulting filter efficiency.

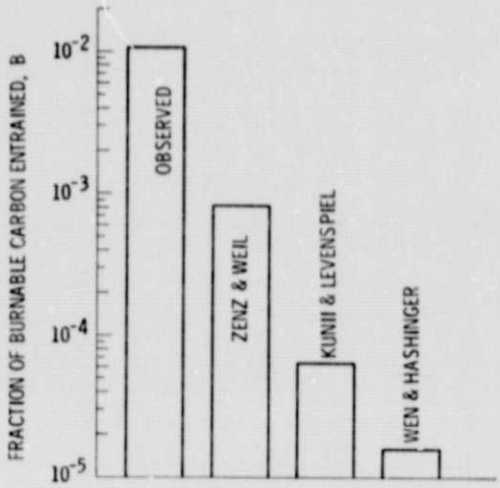

Figure 10 Comparison of burnable carbon entrained based on experiment and three elutriation correlations used in the model of Horio, et al. (1977)[7].

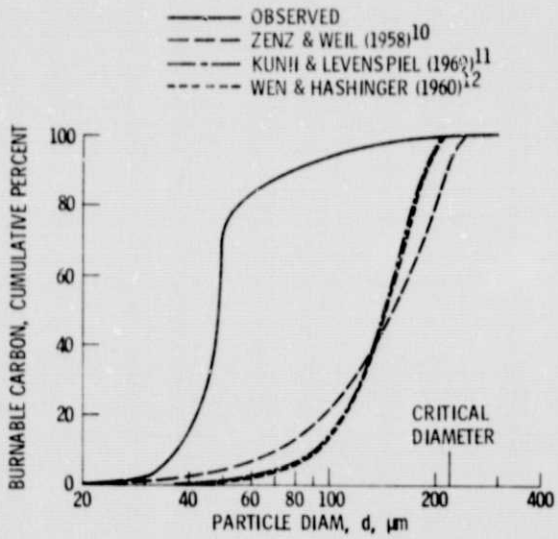

Figure 11 Comparison of calculated and observed size distribution of entrained burnable carbon. All calculations use the model of Horio, et al. (1977)[7] but with different elutriation correlations.

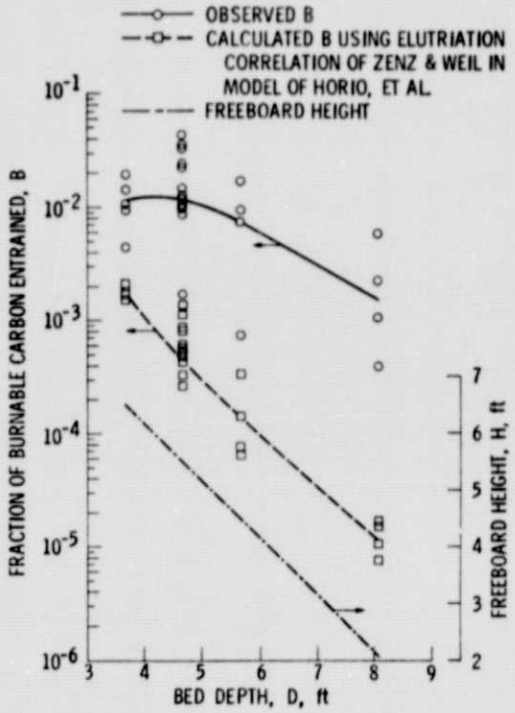

Figure 12 Effect of bed depth on entrained carbon.

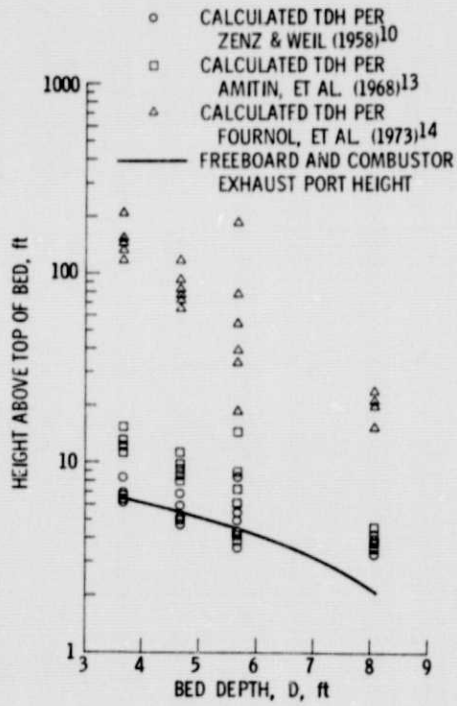

Figure 13 Comparison of calculated transport disengaging height (TDH) with combustor exhaust port height.

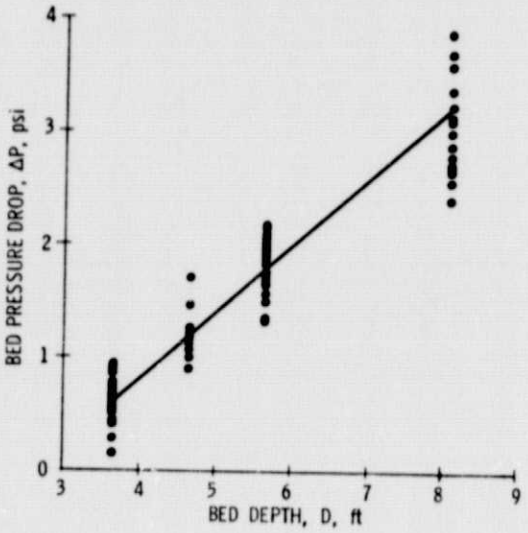

Figure 14 Dependence of bed pressure drop on bed depth.